INSTITUTE OF PHYSICS PUBLISHING SEMICONDUCTOR SCIENCE AND TECHNOLOGY

Semicond. Sci. Technol. **16** (2001) 397–401 www.iop.org/Journals/ss PII: S0268-1242(01)19332-6

Modification of the Si amorphization process by *in situ* ultrasonic treatment during ion implantation

B Romanyuk[1], V Melnik[1], Ya Olikh[1], V Popov[1] and D Krüger[1,2]

[1] Institute for Semiconductor Physics of the Ukrainian Academy of Science, Prospekt Nauki 45, 252028 Kiev, Ukraine

[2] IHP, Frankfurt (Oder), Im Technologiepark 25, 15236 Frankfurt (Oder), Germany

Received 23 November 2000, accepted for publication 7 March 2001

Abstract

We report the first study of the effect of *in situ* ultrasound treatment (UST) during ion implantation on amorphization of crystalline silicon. Rutherford backscattering spectroscopy, ion channelling and cross-section transmission electron microscopy measurements show that amorphization of Si during Ar ion implantation is enhanced by UST, especially at ultrasound frequencies around 2 MHz. The influence on the amorphization process depends mainly on ion flux, ion masses and ultrasound frequency. For implantation conditions without amorphization, for example in the case of implantation with light atoms such as boron, defect concentrations are lower for wafers implanted with UST compared to reference wafers implanted without UST. The influence of ultrasound is discussed in terms of its interaction with point defects and ultrasound-stimulated enhanced diffusion of interstitials.

1. Introduction

Implantation-induced amorphization is widely used to reduce channelling tails of dopant profiles during integrated circuit manufacturing. Amorphization of silicon plays an important role in doping profile formation, influencing also the type and concentration of defects remaining after subsequent thermal annealing. Amorphization processes are also of fundamental interest for radiation physics of solids. Several theoretical models have been proposed to describe different aspects of the amorphization process, such as the overlap of damaged regions, the out-diffusion of point defects and the deposited energy density (e.g. [1, 2]). Despite numerous studies, a detailed understanding of the crystalline–amorphous phase transformation is still not available. This is related to the necessity to take into account numerous factors, such as ion current densities, ion masses, substrate temperature and the presence of elastic stress and of electric fields.

It has been suggested that ultrasound waves propagating through the semiconductor can affect the generation of point defects and dissociation of defect complexes [3]. Ostapenko *et al* [4] found that ultrasound treatment (UST) enhances the dissociation of FeB pairs in poly-Si, and increases the diffusion length of minority carriers. Recently, a review on ultrasound-stimulated processes in semiconductors was published [5]. It seems to be particularly promising to use UST *in situ* during the implantation process, while the target atoms are still in an excited state and defect complexes are unstable or highly metastable. We presented preliminary results on this topic in [6].

Here we report *in situ* ultrasonic modification of the amorphization process in Si during ion implantation. We show that the defect density in the surface layer and thickness of the amorphous layer increase with UST. We explain the results through the interaction of ultrasound with point defects, taking into account enhanced diffusion of interstitials and UST-stimulated formation of vacancy complexes.

2. Experiment

(100) boron-doped, Cz silicon samples ($\rho = 10\ \Omega$ cm) were mounted inside the implantation chamber on piezoelectric transducers via acoustic binders. Low-amplitude ultrasound vibrations were generated in the wafer by operating the transducer in a resonance vibration mode. The basic resonance frequency was varied from 600 kHz to 7 MHz. The amplitude of the generated deformation did not exceed 10^{-5} of the lattice constant, corresponding to an acoustic power of 1 W cm^{-2}. In several experiments the ultrasonic waves in the sample were generated by the incident ion beam itself, without external stimulation ('passive' UST) from the ultrasound generator.

Table 1. Thickness of buried amorphous and near-surface crystalline layers as obtained from RBS after 150 keV Ar^+ implantation at 20 °C for different ultrasound frequencies and current densities.

Sample number	f_{UST} (MHz)	J (μA cm^{-2})	Thickness of a-Si layer (nm)	Thickness of the crystalline surface layer (nm)
62a	—	0.1	172	35.4
62	2	0.1	209	7.9
65	2	0.5	240	0
67	7	0.5	201	28.0

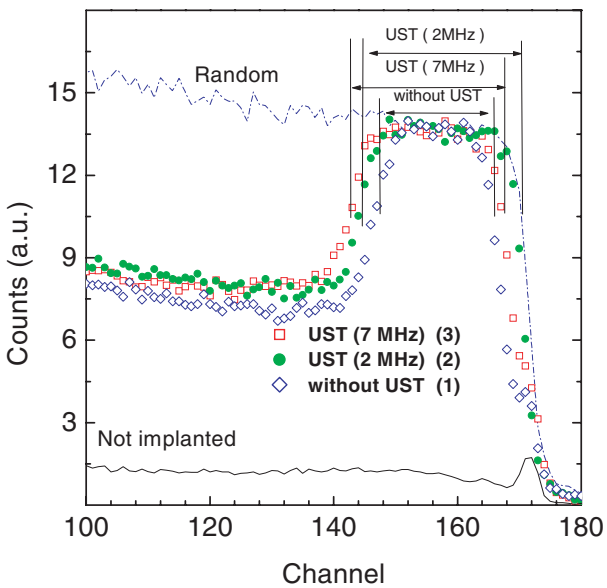

Figure 1. 1.5 MeV He ion RBS channelling spectra of (100) Si samples implanted with Ar ions at a dose of 4×10^{14} cm^{-2}. Curve (1): spectra for implantation without UST. Curves (2), (3): with UST at $f_{UST} = 2$ and 7 MHz, respectively. For comparison a random spectrum and the channelling of an untreated crystal are shown.
(This figure is in colour only in the electronic version, see `www.iop.org`)

This is possible in the case of high implantation doses and high fluxes (more than 1×10^{12} ions cm^{-2} s).

For implantation we used ions of different masses ($^{40}Ar^+$ and $^{11}B^+$) with energies from 50 to 150 keV and doses between 1×10^{13} and 1×10^{16} cm^{-2}. The ion flux was varied from 6×10^{10} to 3×10^{12} ions cm^{-2} s. Damage accumulation was monitored by Rutherford backscattering (RBS) and channelling (RBS-C) using 1.5 MeV He ions at a scattering angle of 170°. The nature of damage was analysed by cross-section transmission electron microscopy (XTEM) before and after rapid thermal annealing at 900 °C.

The implanted structures were studied by Raman spectroscopy (RS) with the spectra excited by an Ar laser (514.5 nm) and measured by an automated instrument developed on the basis of a DFS-24 spectrometer.

3. Results

Figure 1 shows RBS-C spectra for samples implanted with 150 keV Ar^+ at 20 °C to a total dose of 4×10^{14} cm^{-2}. The corresponding samples were implanted without an ultrasound transducer (curve 1), or with ultrasound transducers with resonance frequencies of 2 MHz (curve 2) and 7 MHz (curve 3). The use of ultrasound transducers increases the thickness of the amorphous layer. A movement of the crystalline–amorphous (c–a) interfaces is observed. Correspondingly, the thickness of the amorphous layer is larger in the ultrasound-treated samples, in agreement with the RBS-C results. While a buried amorphous layer with a crystalline layer at the surface is formed in wafers implanted without UST, samples with UST (2 MHz) show a continuous amorphous layer up to the surface. Figure 1 also shows the random and channelling spectra for an untreated sample. The thicknesses of the characteristic layers for different samples are presented in table 1.

With passive UST, the thickness of the amorphous layer increases with increasing ion current density. Without UST, over the temperature range of 25–50 °C and flux range of 10^{11}–10^{13} ions cm^{-2} s, such an increase is not observed. For current densities below 0.01 μA cm^{-2}, no influence of the UST on the amorphization was found. Without an acoustic binder between sample and transducer the UST effects completely vanish.

For $f_{UST} = 2$ MHz the amorphous layer reaches the surface, whereas for $f_{UST} = 7$ MHz only small displacements (about 20 nm) of the inner a–c interface towards the Si bulk is observed. Active ultrasound transducers also enhance the amorphization process.

In figure 2 a bright-field XTEM micrograph of a sample implanted without UST (figure 2(*a*)) is compared with that of a UST sample at $f_{UST} = 2$ MHz (figure 2(*b*)). Afterwards both wafers were annealed at 900 °C for 30 s (figures 2(*c*), (*d*)). For the sample implanted without UST, a buried amorphous layer with a crystalline surface layer is observed. UST with a transducer at $f_{UST} = 2$ MHz creates an a-Si layer reaching the surface. At the a–c interfaces a transition layer about ~40 nm thick, characterized by a high density of defects, is observed in the reference samples. After annealing, typical end-of-range defects (EORDs) are detected. Consequently, for UST different defect structures appear. However, more work is necessary to specify the differences after annealing.

Raman spectra for Si samples implanted with Ar^+ ions under UST of different frequencies are presented in figure 3. We note that the maxima located at 521 and 480 cm^{-1} originate from crystalline and amorphous phases in silicon, respectively [7]. These maxima of the spectra correspond to phonon scattering near the centre of the Brillouin zone in the crystalline phase (peak at 521 cm^{-1}) and to scattering on phonons with random wavevectors in the amorphous phase in the region of ~480 cm^{-1}. A comparison of the spectra shows that the UST leads to a decrease of the crystalline fraction and to an increase of the amorphous one. The frequency dependence was found to be non-monotonic. The most effective influence on the amorphization processes during implantation is obtained with an ultrasound transducer at $f_{UST} = 2$ MHz. Additionally, we found a shift of the maximum at 521 cm^{-1} towards lower

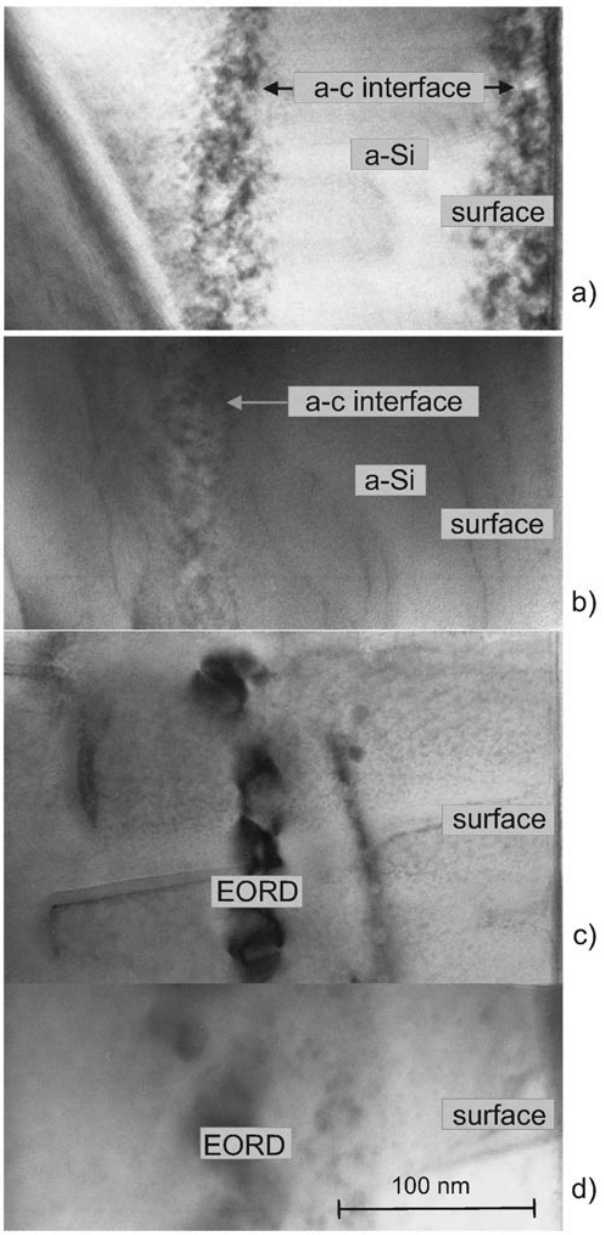

Figure 2. XTEM micrographs of as-implanted silicon samples with 150 keV Ar^+ (*a*) without and (*b*) with UST ($f_{UST} = 2$ MHz); (*c*), (*d*) after annealing at 900 °C for 30 s without and with UST, respectively.

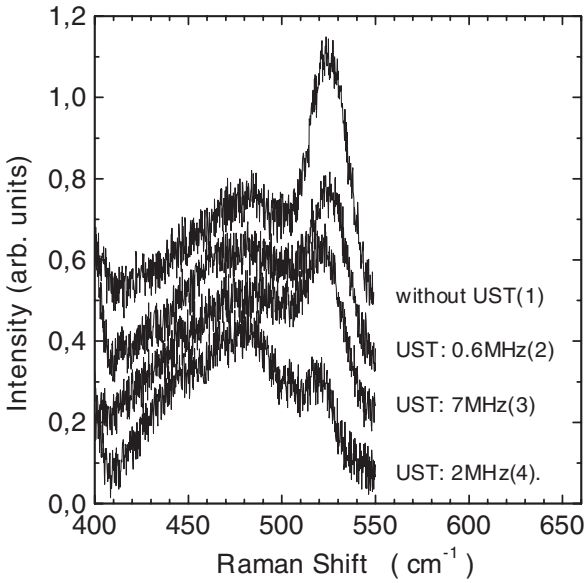

Figure 3. Raman spectra from as-implanted Si samples (150 keV Ar^+, 4×10^{14} cm^{-2}) without UST (1), with UST at $f_{UST} = 0.6$ MHz (2), with UST at $f_{UST} = 7$ MHz (3) and with UST at $f_{UST} = 2$ MHz (4).

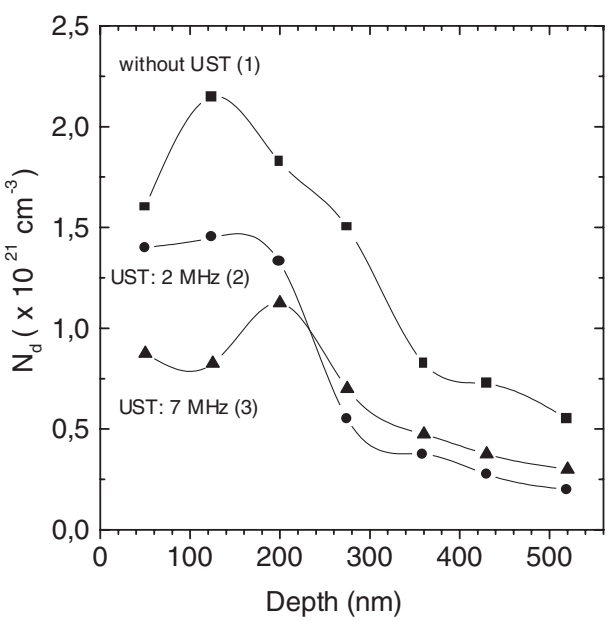

Figure 4. Concentration of displaced atoms versus depth for samples implanted with 50 keV B^+, without UST (curve (1)), with UST at $f_{UST} = 2$ MHz (2), and with UST at $f_{UST} = 7$ MHz (3), obtained from RBS-C data.

energy caused by tensile strain (about 5.5×10^8 N m^{-2}) for $f_{UST} = 2$ MHz. In samples without UST an implantation-induced shift towards compressive strain is detectable.

We have also investigated the influence of UST on the implantation process for light atoms such as boron and carbon. In this case no complete amorphization is achieved for room-temperature implantation. Results for boron implantation are presented below. The implanted B^+ dose was about 1×10^{16} cm^{-2}. In figure 4, the number of displaced Si and B atoms (N_d) is shown for 50 keV B^+-implanted Si wafers without (curve 1) and with UST (curves 2, 3). N_d was determined by measuring the area under the channelling peaks in the RBS spectra [11]. All three curves represent the as-implanted case. For the reference samples implanted without UST, the defect distribution reveals a maximum near R_p. For the samples treated with a frequency $f_{UST} = 7$ MHz (curve 3), a shift of the maximum towards the bulk is observed. For $f_{US} = 2$ MHz the defect distribution saturates in a layer 50–200 nm thick. The defect concentration is lower for wafers implanted with UST (curves 2, 3) compared to the samples with no UST (curve 1). After annealing, samples with UST show a reduced defect density compared to reference samples without UST (figure 5).

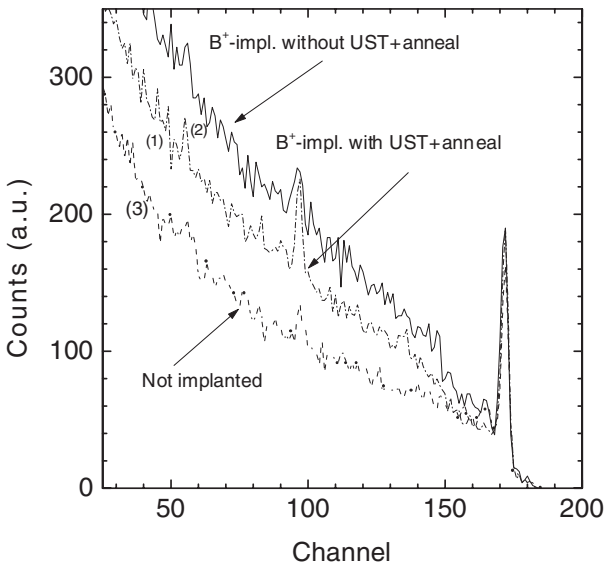

Figure 5. 1.5 MeV He ion RBS channelling spectra of (100) Si samples implanted with B ions at a dose of 1×10^{16} cm^{-2} after annealing at 900 °C for 30 s, implantation with (spectrum (1)) and without UST (spectrum (2)). For comparison a non-implanted reference sample is also shown (spectrum (3)).

4. Discussion

We propose that ultrasound-induced enhanced amorphization can be modelled in terms of ultrasound-stimulated diffusion of interstitials, decreased point defect recombination and kinetic changes in vacancy complex formation. In the case of Ar^+ implantation, every ion creates a disordered area with a diameter of about 3–6 nm. Subsequently, cascade cooling, partial recombination of point defects and creation of point defect complexes take place [8,9]. If the implantation dose increases, amorphous areas are created, and grow by absorption of point defects. Finally, they overlap, forming a continuous amorphous layer.

The presence of ultrasound waves with a moderate intensity (0.1 to 1.0 W cm^{-2}) over the frequency 0.6–7 MHz in the crystal lattice generates substantially less energy compared to the energy deposited in the lattice by the incident ion beam. Therefore, UST should not influence the point defect generation process itself.

Our experiments indicate that ultrasound excitation during ion implantation increases the amorphous layer thickness and reduces the critical amorphization dose. Obviously, ultrasound excitation under non-equilibrium conditions of ion irradiation causes crucial changes. In the absence of ion irradiation we could not detect any changes in the crystal from the sound field alone.

UST at 2 MHz results in a movement of the outer a–c interface towards the surface, where usually vacancy defects are accumulated. We assume, in analogy with ultrasound gas bubble cavitation in liquids [10], that during implantation UST stimulates the following processes: (i) coupling of vacancies into complexes; (ii) tension–compression of 'vacancy bubbles' under ultrasound waves, resulting in their deformation, growth and movement to the surface, and (iii) formation of Ar bubbles. These processes enhance the overlapping of disordered regions and stimulate the formation of a continuous amorphous layer up to the surface.

We assume that ultrasound at lower frequencies (e.g. below 2 MHz) influences mainly the formation of large defect complexes, which are located near the surface. Ultrasound at higher frequencies (e.g. above 7 MHz) seems to influence mainly point defect diffusion. Absorption of phonons generated by the ultrasound wave with frequencies in the range 0.6–7 MHz by the lattice will lead to a small lowering of the activation energy for diffusion [11]. However, the low-frequency ultrasound wave can also excite high-frequency phonons as a result of nonlinear processes. Absorption of these phonons seems to be significant for diffusion enhancement. The excitation of high-frequency phonons can be effectively performed by the incoming ion beam. In the case of 'passive' UST, the ion beam itself generates ultrasound waves in the substrate. With the help of the transducer these waves can be transformed into high-frequency phonons. This process includes not only frequency and phase transformation of the radiation-generated elastic waves, but also multiple reflection, interference phenomena and possible amplitude amplification. These amplified ultrasound waves generate high-frequency phonons, enhancing point defect diffusion.

Experiments on the influence of UST on diffusion should be performed with light atoms. In this case only single point defects are created along the ion tracks without a significant overlap of damaged regions [12, 13]. Our experiments with boron implantation under UST show that the removal of the most mobile interstitial atoms from the implanted region leads to decreasing densities of scattering centres (figure 4, curves 2 and 3). This effect is more pronounced for UST at higher frequencies (7 MHz, shift of the maximum in curve 3). Our results on annealed B-implanted samples show a decrease of the defect density, especially in regions with B. Thus, UST seems to promote better substitutional incorporation of B.

Work is in progress to investigate the influence of *in situ* UST during ion implantation on B diffusion in doping superlattice structures [14].

5. Conclusions

We have investigated the effect of *in situ* UST during ion implantation on amorphization of crystalline silicon. Appropriate UST enhances amorphization of Si during Ar implantation, especially at lower frequencies (below 2 MHz). The effect depends on ion flux, ultrasound frequencies and ion masses. In the case of implantation of light atoms, the defect concentration is lower for wafers implanted with UST compared with reference samples. The experimentally observed effects are discussed in terms of ultrasound-stimulated enhanced point defect diffusion, interaction and clustering.

Acknowledgments

This paper was supported by the BMBF project 01 M 2976. We greatly appreciate the support of V Yuchimchuk, A Franzkevich and R Kurps. We thank Professor A Ourmazd and K Pressel for helpful discussions.

References

[1] Dennis J R and Hale E B 1978 *J. Appl. Phys.* **49** 1119
[2] Gibbons J F 1972 *Proc. IEEE* **60** 1062
[3] Ostrovskij I V and Lisenko V N 1982 *Sov. Phys.–Solid State* **24** 682
[4] Ostapenko S, Jastrebskij L and Sopori B 1995 *Semicond. Sci. Technol.* **10** 1494
[5] Ostapenko S 1999 *Appl. Phys.* A **69** 225
[6] Romanyuk B, Krüger D, Melnik V, Olikh Ya, Popov V, Soroka V and Oberemok O 2000 *Semicond. Phys. Quantum Electron Optoelectron.* **3** 59
[7] *Landolt-Börnstein New Series* Group III, vol 17 (Berlin: Springer) p 390
[8] Goldberg R D, Williams J S and Elliman R G 1995 *Nucl. Instrum. Methods* B **106** 242
[9] Götz G, Glaser E, Wesch W and Sobolev N 1979 *Proc. Int. Conf. on Radiation Physics of Semiconductors (Tiflis)* p 391
[10] Price C J (ed) 1982 *Current Trends in Sonochemistry* (London: Royal Society of Chemistry)
[11] Arakelyan V and Avakyan A 1983 *Phys. Status Solidi* **80** K71
[12] Chu W K, Mayer J W and Nicolett M A 1977 *Backscattering Spectrometry* (New York: Academic Press)
[13] Vos M, Boerma D O, Smulders, P J M and Oosterhoff S 1986 *Nucl. Instrum. Methods* B **180** 234
[14] Krüger D *et al J. Vac. Sci. Technol.* at press